DEPARTMENT OF DEFENCE
DEFENCE SCIENCE & TECHNOLOGY ORGANISATION
DSTO

A Correlation between Flight-determined Longitudinal Derivatives and Ground-based Data for the Pilatus PC 9/A Training Aircraft in Cruise Configuration

Andrew D. Snowden, Hilary A. Keating,
Nick van Bronswijk and Jan S. Drobik

DSTO-TR-0937

A Correlation between Flight-determined Longitudinal Derivatives and Ground-based Data for the Pilatus PC 9/A Training Aircraft in Cruise Configuration

Andrew D. Snowden, Hilary A. Keating, Nick van Bronswijk and Jan S. Drobik

Air Operations Division
Aeronautical and Maritime Research Laboratory

DSTO–TR–0937

ABSTRACT

A series of flight tests were conducted on the PC 9/A aircraft, A23-045, at the Royal Australian Air Force's Aircraft Research and Development Unit. System identification techniques were applied to the data obtained from these flight tests to determine the stability and control derivatives of the aircraft. The longitudinal results for the aircraft in cruise configuration are presented in this report and comparisons are made with empirical and ground based estimates.

Published by

DSTO Aeronautical and Maritime Research Laboratory
506 Lorimer St,
Fishermans Bend, Victoria, Australia 3207

Telephone: (03) 9626 7000
Facsimile: (03) 9626 7999

AR No. AR-011-205
February, 2000

APPROVED FOR PUBLIC RELEASE

A Correlation between Flight-determined Longitudinal Derivatives and Ground-based Data for the Pilatus PC 9/A Training Aircraft in Cruise Configuration

EXECUTIVE SUMMARY

Air Operations Division (AOD) has developed, or acquired, a number of fixed-wing flight dynamic models and is also responsible for providing advice to the Australian Defence Organisation (ADO) on flight simulator flight dynamic model requirements. The models generally make use of extensive static and dynamic stability and control derivative databases, in addition to engine and flight control models. The static model data may be obtained from wind tunnel testing, whilst the dynamic data is traditionally obtained from flight tests using system identification techniques.

The system identification techniques used to estimate aerodynamic derivatives of conventional aircraft are well established. The major requirement of these techniques is high fidelity measurements of manoeuvre input (i.e. control surface deflections), and aircraft response (i.e. angular rates and linear accelerations), as well as air data including airspeed, altitude, angle-of-attack and angle-of-sideslip.

Following the completion of the AOD PC 9/A wind tunnel tests, the requirement existed for a dedicated flight dynamic modelling flight test program to both validate the flight dynamic model of the PC 9/A and to provide dynamic derivative estimates which were unobtainable in the AMRL wind tunnel. An instrumentation suite, including an air data probe for the direct and accurate measurement of angle-of-attack, angle-of-sideslip, temperature, and static and dynamic pressure, was fitted to the aircraft and a test manoeuvre matrix was designed specifically for the purpose of gathering flight dynamic data. This flight test program was conducted at the Aircraft Research and Development Unit (ARDU) during 1998/99.

This report details the analysis of the longitudinal manoeuvres carried out with the aircraft in the cruise configuration. The static and dynamic derivatives thus obtained are compared with wind tunnel estimates as well as a number of empirical estimates obtained from alternative sources. A discussion of some of the difficulties encountered during the estimation process is also included. The data obtained from these tests will be used in the development of the PC 9/A flight dynamic model for the purpose of enhancing AOD support for the PC 9/A fleet, including possible upgrades to the part-task trainer.

Authors

Andrew Snowden
Air Operations Division

Andrew Snowden graduated from the Royal Melbourne Institute of Technology in 1991, having obtained a Bachelor of Engineering in Aerospace Engineering with first class honours. Before commencing work at AMRL he served a short term attachment with McDonnell Douglas in St. Louis, Missouri, as the recipient of the McDonnell Aircraft Company Aerospace Engineering Prize for 1991. He commenced employment at AMRL in 1992 and participated in several experimental investigations in a number of different fields during his rotation. Now a full time member of the flight dynamics and performance area of the Air Operations Division, his most recent work includes the organisation of flight testing for parameter identification of the Pilatus PC 9/A as well as performance estimation of modern jet fighters.

Hilary Keating
Air Operations Division

Hilary Keating graduated from the University of Sydney in 1998, having obtained a Bachelor of Engineering in Aeronautical Engineering with first class honours. She commenced employment at AMRL in 1999, and has been involved in performance modelling and parameter identification of the Pilatus PC 9/A.

Nick van Bronswijk
Air Operations Division

Nick van Bronswijk graduated from the University of Sydney with first class honours in Aeronautical Engineering in 1995. He is currently completing his PhD in the area of propeller power effects. Since joining AMRL in 1998 he has been involved with a range of projects including flight and wind tunnel test programs of the Pilatus PC 9/A.

Jan Drobik
Air Operations Division

Jan Drobik leads a team that is responsible for the implementation of solutions to flight dynamic problems which arise throughout the ADF's fleet of aircraft. Since joining the then ARL in 1978, he has acquired broad experience in the areas of flight dynamics and experimental aerodynamics. He has been responsible for the development of aircraft flight dynamic models and aerodynamic parameter estimation techniques within AMRL, and has managed its successful application to a wide range of practical problems. He has been involved in TTCP activities in AER Technical Panel AER TP–5 for many years, becoming Australian National Leader in 1998.

Contents

Appendices

Figures

Tables

Glossary

AHRS	Artificial Horizon Reference System
AMRL	Aeronautical and Maritime Research Laboratory
AOD	Air Operations Division
ARDU	Aircraft Research and Development Unit
DSTO	Defence Science and Technology Organisation
GDAS	General Data Acquisition System
IAS	Indicated Airspeed
ITT	Inlet Turbine Temperature
KIAS	Knots Indicated Airspeed
MAC	Mean Aerodynamic Chord
NASA	National Aeronautics and Space Administration
NG	Gas generator speed
OAT	Outside Air Temperature
PAP	Primary Analysis Processor
RAAF	Royal Australian Air Force
SHP	Shaft Horse Power

Notation

a_X, a_Y, a_Z	Body axes linear accelerations (g)
b	Reference span (10.124 m)
C_m	Pitching moment coefficient $C_m = \frac{m}{\bar{q}S\bar{c}}$
C_{m_α}	Pitching moment coefficient due to angle-of-attack $C_{m_\alpha} = \frac{\partial C_m}{\partial \alpha}$ (per degree)
$C_{m_{\dot{\alpha}}}$	Pitching moment coefficient due to rate of change of angle-of-attack $C_{m_{\dot{\alpha}}} = \frac{\partial C_m}{\partial\left(\frac{\dot{\alpha}\bar{c}}{2V}\right)}$ (per radian)
$C_{m_{\delta_e}}$	Pitching moment coefficient due to elevator deflection $C_{m_{\delta_e}} = \frac{\partial C_m}{\partial \delta_e}$ (per degree)
C_{m_q}	Pitching moment coefficient due to pitch rate $C_{m_q} = \frac{\partial C_m}{\partial\left(\frac{q\bar{c}}{2V}\right)}$ (per radian)
C_N	Normal force coefficient $C_N = \frac{N}{\bar{q}S}$
C_{N_α}	Normal force coefficient due to angle-of-attack $C_{N_\alpha} = \frac{\partial C_N}{\partial \alpha}$ (per degree)
$C_{N_{\dot{\alpha}}}$	Normal force coefficient due to rate of change of angle-of-attack $C_{N_{\dot{\alpha}}} = \frac{\partial C_N}{\partial\left(\frac{\dot{\alpha}\bar{c}}{2V}\right)}$ (per radian)
$C_{N_{\delta_e}}$	Normal force coefficient due to elevator deflection $C_{N_{\delta_e}} = \frac{\partial C_N}{\partial \delta_e}$ (per degree)
C_{N_q}	Normal force coefficient due to pitch rate $C_{N_q} = \frac{\partial C_N}{\partial\left(\frac{q\bar{c}}{2V}\right)}$ (per radian)
C_X	Longitudinal force coefficient $C_X = \frac{X}{\bar{q}S}$
C_Z	Vertical force coefficient $C_Z = \frac{Z}{\bar{q}S}$
$\bar{c}$	Reference chord (1.65 m)
F	Ratio of the regression mean square to the residual mean square
g	Gravitational acceleration (9.81 m/s^2)
I_{XX}	Roll moment of inertia (kg.m^2)
I_{YY}	Pitch moment of inertia (kg.m^2)
I_{ZZ}	Yaw moment of inertia (kg.m^2)
I_{XY}	Cross product of moment of inertia (kg.m^2)
I_{XZ}	Cross product of moment of inertia (kg.m^2)
I_{YZ}	Cross product of moment of inertia (kg.m^2)
M	Mass of aircraft (kg)
m	Pitching moment (N.m)
N	Normal force (N)
p	Roll rate (rad/s)
q	Pitch rate (rad/s)
$\bar{q}$	Dynamic pressure (N/m^2)

R^2	Squared multiple correlation coefficient
r	Yaw rate (rad/s)
S	Reference area (16.29 m^2)
V	True velocity (m/s)
X	Longitudinal force (N)
$x_{c.g.}$	Longitudinal *c.g.* position (m)
$y_{c.g.}$	Lateral *c.g.* position (m)
Z	Vertical force (N)
$z_{c.g.}$	Vertical *c.g.* position (m)
α	Angle-of-attack (°)
$\dot{\alpha}$	Time derivative of angle-of-attack (rad/s)
β	Angle-of-sideslip (°)
δ_a	Aileron deflection ($\delta_a = \delta_{a_L} - \delta_{a_R}$) (°)
δ_e	Elevator deflection (°)
δ_r	Rudder deflection (°)
θ	Pitch angle (°)
ϕ	Roll angle (°)
ψ	Yaw angle (°)

Subscripts

b	Body axes
c.g.	Centre of gravity
F	Fuel
L	Left (port)
R	Right (starboad)

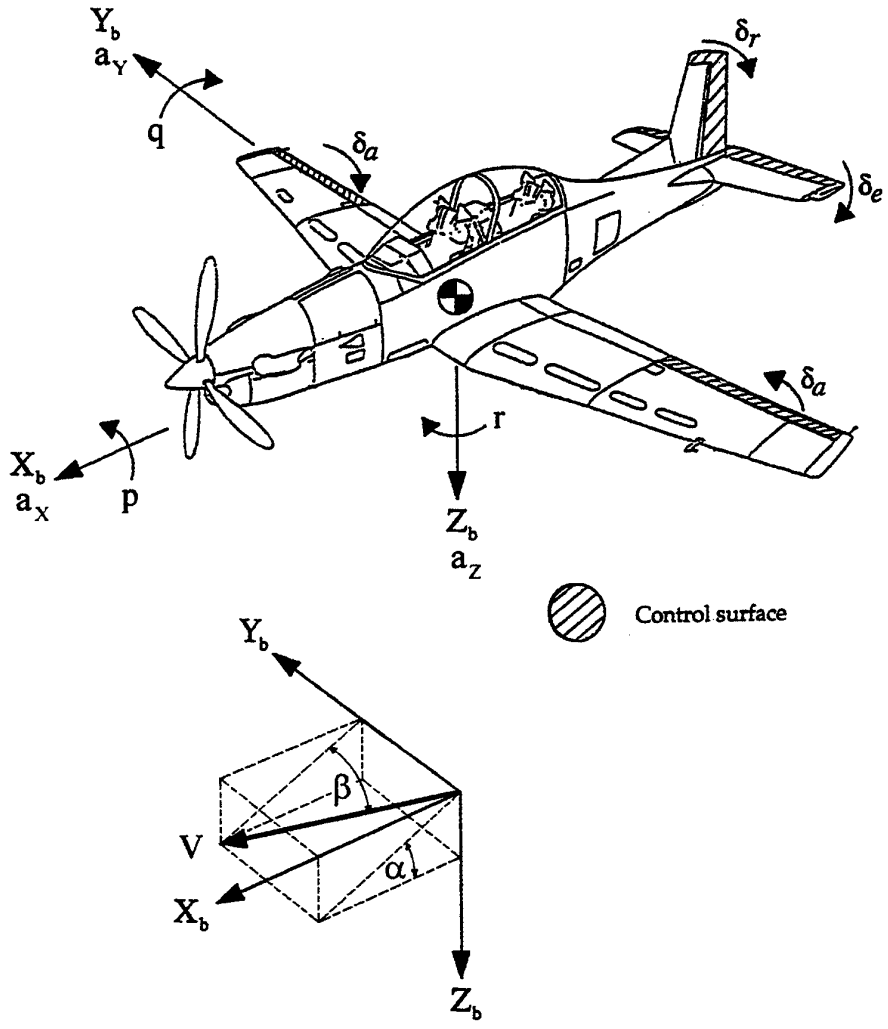

Aircraft sign convention and flow angle definitions (body axes).

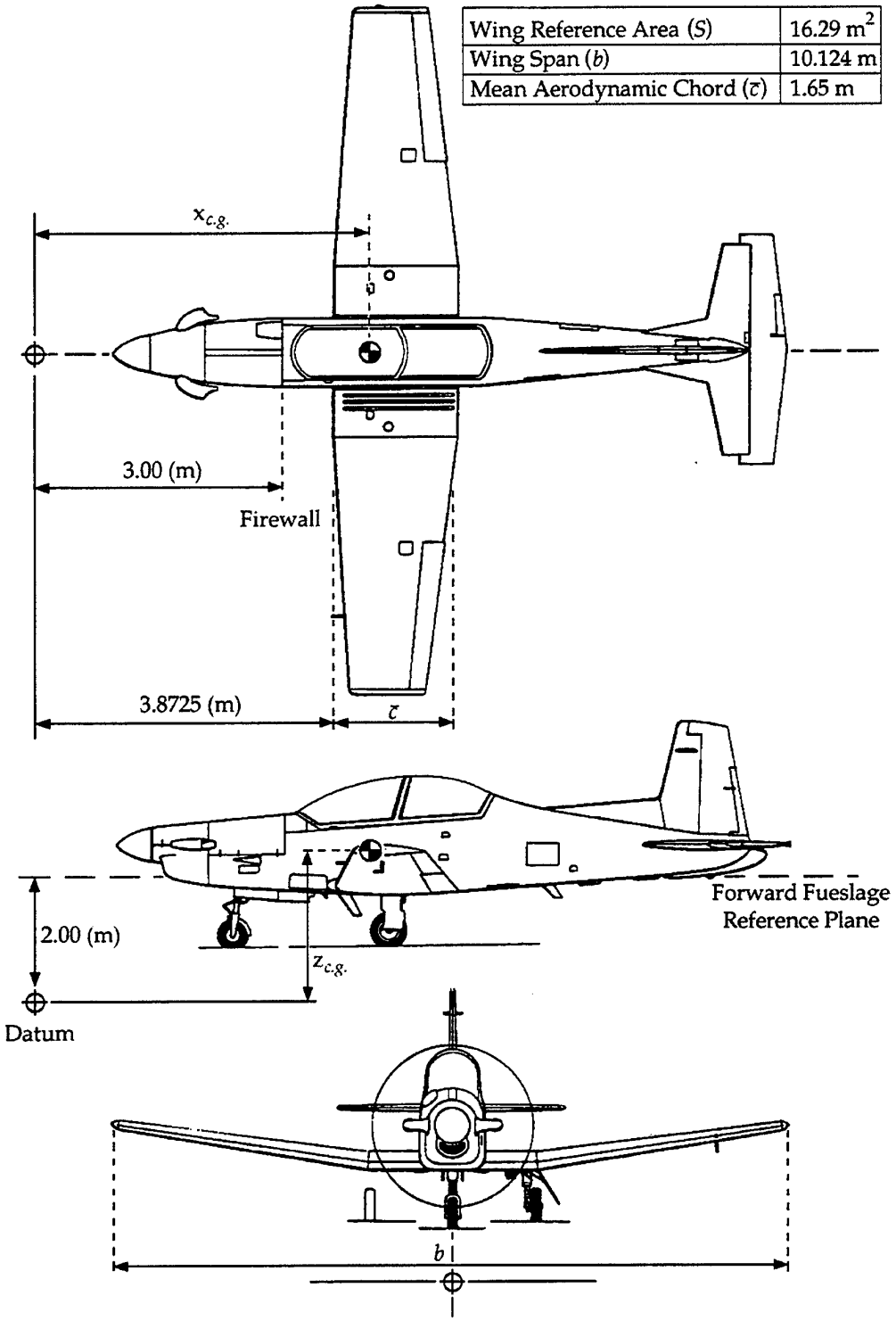

Aircraft Principle Dimensions.
(Numeric data sourced from Pilatus Structural Configuration Drawing 506.00.09.220F)

1 Introduction

The Pilatus PC 9/A is one of a number of high performance turbo-prop aircraft currently operated by the Royal Australian Air Force (RAAF). Work currently underway in the Air Operations Division (AOD) of the Defence Science and Technology Organisation (DSTO) includes investigations into the propeller power effects of such aircraft, and the PC 9/A was considerd a suitable platform for study. A six degree-of-freedom flight dynamic model of the PC 9/A has been developed by AOD for use in these investigations, as well as for pilot-in-the-loop simulations in the Air Operations Simulation Centre and incident and accident investigations.

The development of a flight dynamic model requires information on the static and dynamic stability and control derivatives of the aircraft, as well as flight control laws and physical properties. The static data for the PC 9/A were collected during both power-off and power-on testing of a scaled aircraft model in the Aeronautical and Maritime Research Laboratory (AMRL) low-speed wind tunnel. Additional power-off static data were obtained from a computational fluid dynamic model for a limited number of aircraft configurations.

Flight test data for the PC 9/A was required to both validate the flight dynamic model and to provide dynamic derivative estimates of the aircraft. A flight test program was conducted on a PC 9/A aircraft, serial number A23-045, by the RAAF Aircraft Research and Development Unit (ARDU) between November 1998 and February 1999. The details of this flight test program and the aircraft instrumentation are reported in reference [1]. The estimation of the stability and control derivatives from the flight test data involved the use of system identification techniques, and required control input, aircraft response and flight condition data, measured using a high fidelity instrumentation system. Maximum likelihood and stepwise regression techniques were employed for the system identification.

This report presents the longitudinal stability and control derivatives of the PC 9/A extracted from flight test data for the cruise configuration, including a comparision with AMRL wind tunnel test data and empirical results. Sections 2 and 3 present details of the test aircraft and instrumentation system. Section 4 presents the system identification techniques, while section 5 discusses the results.

2 PC 9/A Test Aircraft

2.1 Aircraft Description

The flight test aircraft, A23-045 is a Pilatus PC 9/A operated by ARDU. The PC 9/A is a single-engine, metal-skinned, low-wing, tandem two-seat training aircraft. The aircraft is powered by a Pratt and Whitney PT6A-62 turbo-prop engine flat rated to 950 SHP [2], which drives a Hartzell HC-D4N-2A four-blade variable pitch propeller. The aircraft was instrumented as outlined in section 3.

2.2 Flight Control System

The aircraft primary flight controls consist of the ailerons, rudder and elevator. The control surfaces are manually operated from a conventional dual control column and rudder pedal arrangement. The stick and rudder pedals are connected to the control surfaces through a system of control rods, bellcranks, cables and levers. Trimming control is provided on all three axes.

2.3 Weight, Centre-of-Gravity and Mass Moments-of-Inertia

The test aircraft, A23-045, was weighed by ARDU prior to the flight tests and had a basic mass of 1784.5 kg and a longitudinal centre-of-gravity position of 26.25%MAC [3]. During the flight test program, the aircraft weight, centre-of-gravity and mass moments-of-inertia varied with fuel usage. These parameters were calculated for each test manoeuvre using the equations in Appendix A.

3 Instrumentation

Aircraft A23-045 was fitted with an instrumentation system designed specifically for the gathering of flight dynamic data. A summary of the instrumentation used in the flight test program is included below and a more comprehensive description of the design requirements and calibration is included in references [1] and [4]. The ARDU General Data Acquisition System (GDAS) was fitted in place of the rear ejection seat. The data were encoded by a 16-bit pulse code modulation system and were recorded onboard the aircraft using a MARS-2000 14-track tape. Real-time flight test monitoring was provided by telemetry data transmitted to the ARDU Primary Analysis Processor (PAP) hut.

The angular rates (p, q, r) and linear accelerations (a_X, a_Y, a_Z) were measured using the ARDU KAISG1134-1 Motion Platform. This consisted of three Smith Industries 950 RGS angular rate gyros and three SunStrand QA1400 servo accelerometers. The aircraft roll, pitch and yaw attitude angles (ϕ, θ, ψ) were obtained by tapping output from the existing LISA 2000A Artificial Horizon Reference System (AHRS).

Static outside air temperature (OAT), indicated airspeed (IAS), angle-of-attack (α) and angle-of-sideslip (β) were obtained from the Rosemount Model 92AN flight test air data boom, mounted on the outboard hardpoint on the starboard wing (see figure 1). Aileron and elevator deflections were measured using Space Age Control Inc. series 160 cable position transducers. Rudder deflection was measured using a type 26V-11CX4C position transducer. All sensors were calibrated prior to commencement of the flight test program.

The aircraft was also instrumented to measure engine torque, propeller speed, inlet turbine temperature (ITT), gas generator speed (NG), fuel flow and fuel quantity. The torque, propeller speed, altitude and true airspeed, when used in conjunction with a performance map for the Hartzell HC-D4N-2A propeller [5], allowed the calculation of engine thrust.

4 Methods of Analysis

During the flight test program, doublet and 3-2-1-1 manoeuvres were performed about steady flight conditions at airspeeds between 90 and 200 KIAS. Reference [1] describes these manoeuvres in detail. The 34 longitudinal doublet and 140 longitudinal 3-2-1-1 manoeuvres were analysed using stepwise regression [6] and maximum likelihood estimation techniques [7] to determine the longitudinal stability and control derivatives of the aircraft.

Aircraft derivatives estimated from AMRL power-off wind tunnel tests [8] and empirical data estimated by Pilatus [9] using Digital Datcom [10] [11] were used to provide comparisons and in the case of the maximum likelihood analysis, to provide *a priori* estimates to increase the rate of convergence of the system identification.

A right handed orthogonal axes system was adopted for the analysis of the flight test data. Positive control surface deflections were defined as elevator trailing edge down, rudder trailing edge to port, and starboard aileron trailing edge down, port aileron trailing edge up.

4.1 Stepwise Regression

Stepwise regression is an unbiased least squares estimator in which new independent variables are inserted into a model, one at a time, until the regression equation is deemed acceptable. The appropriateness of the model can be determined by examining a number of quantities including the squared multiple correlation coefficient and the F statistic. The squared multiple correlation coefficient, R^2, gives a measure of the importance of each variable as it is inserted into the equation [6]; however, the improvement in R^2 due to the addition of new terms must have some real significance besides simply reflecting the inclusion of more terms. This can be determined by monitoring the F statistic, the ratio of the regression mean square to the residual mean square. The inclusion of any significant terms is generally accompanied by an increase in the F statistic and the best fit with the least number of parameters may be obtained by maximising F. Any variable which does not make a significant contribution is removed from the model, with the selection process continuing until no new variables remain to be inserted into the equation. Whilst stepwise regression gives estimates of the derivatives included in the regression equation, it also permits a suitable structure for the model to be determined. In addition, it provides an independent check on the data estimated using the maximum likelihood technique.

The stepwise regression technique was applied using code available in the MATLAB© Statistics Toolbox [12]. The following model equations were identified during the analysis.

$$C_N = C_{N_0} + C_{N_\alpha}\alpha + C_{N_{\delta_e}}\delta_e \tag{1}$$

$$C_m = C_{m_0} + C_{m_\alpha}\alpha + C_{m_q}\frac{q\bar{c}}{2V} + C_{m_{\delta_e}}\delta_e \tag{2}$$

4.1.1 Error Band

Included in the stepwise regression analysis is the calculation of an error band on the estimated derivatives. For a confidence interval of 95%, this error band is approximately equal to two standard deviations. Figures 2 to 11 show the stepwise regression derivative estimates, including the calculated error band.

4.2 Maximum Likelihood

The maximum likelihood estimation technique was applied using the computer program, pEst, developed at NASA Dryden Flight Research Center [13]. pEst is an interactive parameter estimation program which solves a vector set of time-varying, ordinary differential equations of motion.

The longitudinal derivatives identified using the maximum likelihood technique are given in table 1. Three aerodynamic derivatives used in the longitudinal flight dynamic model were not identified due to both their small contribution and difficulty of estimation.

	Normal Force	Pitching Moment
Aerodynamic	C_{N_α}	C_{m_α} C_{m_q}
Control	$C_{N_{\delta_e}}$	$C_{m_{\delta_e}}$

Table 1: Longitudinal derivatives estimated.

The derivative $C_{m_{\dot{\alpha}}}$ is difficult to estimate from standard flight test manouevres and is usually considered as an additional component of the pitch damping derivative C_{m_q} during parameter identification [14]. Experience gained during the analysis of F-111C flight test data [15] has shown that it is preferable to fix $C_{m_{\dot{\alpha}}}$ at it's *a priori* value, chosen here as -7.823 (per radian), and allow C_{m_q} to be estimated.

Difficulties also arise when trying to estimate both the normal force due to pitch rate derivative, C_{N_q}, and the normal force due to the time rate-of-change of angle-of-attack derivative, $C_{N_{\dot{\alpha}}}$. In the case of the PC 9/A, analysis showed that the relative contributions of C_{N_q} and $C_{N_{\dot{\alpha}}}$ to the total aircraft normal force were negligible, and these derivatives could be fixed at their *a priori* values, chosen as 7.96 (per radian) and 3.061 (per radian), respectively, without any loss to the accuracy of the estimation of the other normal force derivatives, C_{N_α} and $C_{N_{\delta_e}}$ (refer appendix B).

The *a priori* values of $C_{m_{\dot{\alpha}}}$, C_{N_q} and $C_{N_{\dot{\alpha}}}$ were obtained from empirical data in reference [9]. The resulting total force and moment coefficient equations used in the state and response equations for the maximum likelihood analysis of the PC 9/A are given in equations 3 and 4. The differences between equations 1 and 2, and 3 and 4 are important, and arise from the inclusion of the *a priori* values in the maximum likelihood technique.

$$C_N = C_{N_0} + C_{N_\alpha}\alpha + 7.96\frac{q\bar{c}}{2V} + C_{N_{\delta_e}}\delta_e + 3.061\frac{\dot{\alpha}\bar{c}}{2V} \tag{3}$$

$$C_m = C_{m_0} + C_{m_\alpha}\alpha + C_{m_q}\frac{q\bar{c}}{2V} + C_{m_{\delta_e}}\delta_e - 7.823\frac{\dot{\alpha}\bar{c}}{2V} \quad (4)$$

4.2.1 Cramer-Rao Bounds

For the estimated parameters, pEst calculates a measure of the estimation certainty known as the Cramer-Rao bound. A detailed interpretation of this quantity is given in [16]. The Cramer-Rao bounds are shown for each derivative estimated by pEst in figures 2 to 11. The Cramer-Rao bounds have been factored in accordance with the procedures described in [16] to account for the presence of band-limited noise.

5 Results and Discussion

Longitudinal derivatives estimated via maximum likelihood parameter estimation, stepwise regression, empirical methods and power-off wind tunnel experiments are summarised in figures 2 to 11.

5.1 Angle-of-Attack Derivatives

Figures 2 to 6 show the angle-of-attack derivatives C_{N_α} and C_{m_α} plotted against α. Flight test estimates, derived from 3-2-1-1 manoeuvres, of the normal force due to angle-of-attack derivative, C_{N_α}, display very good agreement with the wind tunnel estimate from both system identification techniques. The results exhibit a similar variation with angle-of-attack, with C_{N_α} decreasing as α increases, as that predicted by wind tunnel tests. For the doublet manoeuvres, the maximum likelihood estimates fall between the empirical and wind tunnel estimates, whilst the stepwise regression estimates still agree well with the wind tunnel data.

The flight test estimates of the pitch stiffness derivative, C_{m_α}, are generally smaller in magnitude than the wind tunnel and empirical estimates which are both power-off. This difference is due to the imbalance between two competing effects acting on the portion of the horizontal tail within the propeller slipstream, these being the increased dynamic pressure and the reduced angle of incidence. The reduction in angle of incidence dominates, resulting in an overall reduction in the pitch stiffness of the aircraft, as seen in figures 2 to 6. This phenomenon is discussed further in section 5.4. The flight test results exhibit the same variation with angle-of-attack as predicted by the wind tunnel.

5.2 Pitch Rate Derivatives

Figures 2 to 6 show the pitch rate derivative C_{m_q} plotted against α. As discussed earlier, $C_{m_{\dot{\alpha}}}$ was fixed at it's *a priori* value to aid the estimation of the pitch damping derivative C_{m_q}. This method has been used successfully during other parameter estimation

exercises [15], and the results shown in figures 2 to 6 confirm this. In general, the flight test estimates of C_{m_q} from maximum likelihood and stepwise regression agree well with empirical data. The AMRL low-speed wind tunnel has no facility to measure dynamic derivatives. Thus only empirically derived estimates are available for comparison. The flight test estimates exhibit a degree of scatter at angles-of-attack higher than 9°.

Data analysis carried out previously on the PC 9/A and F-111C [15] has consistently highlighted the difficulty of obtaining reasonable estimates for the normal force due to pitch rate derivative, C_{N_q}. In the past, the derivative C_{N_q} was usually fixed at some *a priori* value whilst the remaining derivatives were estimated. The opportunity was taken with the PC 9/A data to further investigate the effect that fixing C_{N_q} would have on the other derivatives. This investigation found that the contributions of both C_{N_q} and $C_{N_{\delta_e}}$ to the total normal force coefficient, C_N, are negligible, hence the effect of any errors present in the *a priori* estimate of C_{N_q} should be minimal. A detailed discussion of this analysis is given in appendix B.

5.3 Control Derivatives

Figures 7 to 11 show the control derivatives $C_{N_{\delta_e}}$ and $C_{m_{\delta_e}}$ plotted against α. The maximum likelihood estimates of $C_{m_{\delta_e}}$ agree well with the wind tunnel estimate, whilst stepwise regression consistently underestimates the magnitude of $C_{m_{\delta_e}}$ in comparison with the wind tunnel estimate. The flight test results also exhibit a reasonable degree of scatter above 9° angle-of-attack. Overall, however, the low Cramer-Rao bounds would indicate a high level of confidence in the maximum likelihood estimates of $C_{m_{\delta_e}}$.

Estimates of $C_{N_{\delta_e}}$ show a high degree of scatter at angles-of-attack above 9° and fall short of both the wind tunnel and empirical estimates. In the case of the stepwise regresion results, negative values of $C_{N_{\delta_e}}$ were observed. As discussed previously, *a priori* values are included in the maximum likelihood technique, whereas the stepwise regression technique does not consider these values. In order to assess the effect of this difference, a number of manoeuvres were analysed using the maximum likelihood technique where the *a priori* values were set to zero. This analysis showed the effect of the *a priori* values on the estimated derivatives to be small. However, a change in sign of $C_{N_{\delta_e}}$ was observed, similar to that seen in the stepwise regression results. It is therefore proposed that the effect of setting both $C_{N_{\dot{\alpha}}}$ and C_{N_q} to zero is to reduce the rate of onset of normal force during a manoeuvre and therefore, the modelling techniques decrease the value of $C_{N_{\delta_e}}$, to below zero, to compensate. This ensures the overall match of the data is good but results in some loss of model resolution during the inital application of elevator.

5.4 Variation of Longitudinal Derivatives with Rate of Climb and Angle-of-Attack

Figure 12 shows the variation of the longitudinal derivatives with angle-of-attack and nominal rate of climb for a selection of 3-2-1-1 manoeuvres. A linear curve fit was applied to each rate of climb data set, to highlight the trends shown by the data. The figure shows that the influence of rate of climb on the longitudinal derivatives increases with increasing

angle-of-attack, with the magnitude of C_{m_α} decreasing (an effective forward movement of the aircraft neutral point), while the magnitudes of C_{m_q} and $C_{m_{\delta_e}}$ increase (due to the increased dynamic pressure in the propeller slipstream). These trends result from the increase in aircraft thrust coefficient with rate of climb at a given angle-of-attack. They are in agreement with previous theoretical and experimental studies detailed in references [17] and [18]. For the manoeuvres in figure 12, thrust coefficient varies from approximately 0.02 to approximately 0.09.

5.5 Manoeuvre Type and Altitude Dependency

Tables 2 and 3 show the mean values across the linear angle-of-attack range (0° - 6°) of the aerodynamic derivatives estimated by both the maximum likelihood and stepwise regression techniques, for each manoeuvre type and altitude band.

	C_{N_α}	$C_{N_{\delta_e}}$	C_{m_α}	C_{m_q}	$C_{m_{\delta_e}}$
3211 5000 ft	8.94E-02	5.50E-03	-7.70E-03	-1.44E+01	-2.15E-02
3211 10 000 ft	8.82E-02	5.40E-03	-7.20E-03	-1.41E+01	-2.12E-02
3211 15 000 ft	8.77E-02	5.00E-03	-7.00E-03	-1.47E+01	-2.12E-02
Doublet 5000 ft	9.18E-02	2.96E-03	-7.74E-03	-1.38E+01	-2.10E-02
Doublet 15 000 ft	8.99E-02	3.60E-03	-7.18E-03	-1.59E+01	-2.18E-02

Table 2: Summary of derivatives estimated using maximum likelihood.

	C_{N_α}	$C_{N_{\delta_e}}$	C_{m_α}	C_{m_q}	$C_{m_{\delta_e}}$
3211 5000 ft	7.78E-02	-3.00E-03	-5.50E-03	-1.93E+01	-1.98E-02
3211 10 000 ft	8.45E-02	-4.30E-03	-5.50E-03	-1.39E+01	-1.67E-02
3211 15 000 ft	7.93E-02	-4.40E-03	-4.80E-03	-1.54E+01	-1.61E-02
Doublet 5000 ft	8.14E-02	-4.90E-03	-6.43E-03	-1.45E+01	-1.61E-02
Doublet 15 000 ft	8.27E-02	-4.44E-03	-6.21E-03	-1.64E+01	-1.73E-02

Table 3: Summary of derivatives estimated by stepwise regression.

The flight test estimates for the 3-2-1-1 and doublet manoeuvres do not show any significant dependency on manoeuvre type. In general, the results show increasing uncertainty bounds and scatter with increasing angle-of-attack. This trend was more evident in the 3-2-1-1 manoeuvres, which were performed over a larger angle-of-attack range. This is not suprising, as at trim angles-of-attack above approximately 9° the aircraft was operating in the non-linear region of the flight envelope. Furthermore, the test pilot reported difficulty in maintaining trim and performing the manoeuvres at these conditions.

As all the derivatives are non-dimensionalised by dynamic pressure, they were expected to be insensitive to the altitude at which the manoeuvre was executed. Figures 2 to 11 confirm this.

6 Conclusions

Derivatives describing the longitudinal stability and control characteristics of the PC 9/A in the cruise configuration were determined from flight test data measurements using maximum likelihood and stepwise regression techniques. The results were compared with power-off wind tunnel and empirical values.

Estimates of the longitudinal stability derivatives, C_{N_α}, C_{m_α} and C_{m_q}, showed reasonable agreement with the corresponding wind tunnel values and empirical estimates. The flight test and wind tunnel results also exhibit similar trends, when plotted against angle-of-attack. Good agreement with wind tunnel and empirical estimates was observed for the longitudinal control derivate, $C_{m_{\delta_e}}$. The results for $C_{N_{\delta_e}}$ showed a high degree of scatter and were affected by the exclusion of *a priori* values in the stepwise regression analysis. Any discrepancies in this derivative should not affect the aircraft model due to its low significance in the total C_N equation.

In general, the flight test derivative estimates did not show any significant dependence on altitude or manoeuvre type. However, they showed larger scatter and possessed larger uncertainty bounds at angles-of-attack above 9°, where the aircraft was operating in the non-linear region of the flight envelope. The longitudinal derivatives C_{m_α}, C_{m_q} and $C_{m_{\delta_e}}$ exhibited trends when plotted as a function of climb rate that were consistent with those predicted by earlier theoretical and experimental studies.

References

1. A. D. Snowden. PC 9/A flight tests summary. Client Report AOD 99/01, Aeronautical and Maritime Research Laboratory, 1999.

2. Royal Australian Air Force. *Flight Manual PC 9/A*. Defence Instruction (Air Force) AAP 7212.007-1, June 1989.

3. M.C. Sciberras. Aircraft weigh record - A23-045. ARDU 2501/60/TechPt1(5), November 1998.

4. B. A. Woodyatt, A. D. Snowden, and K. E. Lillingston. The development of a PC 9/A flight dynamic model validation flight test program. Client Report AOD 98/07, Aeronautical and Maritime Research Laboratory, 1998.

5. British Aerospace. Pilatus PC 9/A performance maps. Technical memorandum, British Aerospace Aerodynamics, Brough.

6. V. Klein. Estimation of aircraft aerodynamic parameters from flight data. *Progress in Aerospace Sciences*, 26:1–77, 1989.

7. R.E. Maine and K.W. Iliff. Application of parameter estimation to aircraft stability and control, the output error approach. Reference Publication 1168, NASA Dryden Flight Research Facility, Edwards, California, USA, June 1986.

8. R. M. Carmichael and B. A. Woodyatt. Estimates of the power-off aerodynamic characteristics of the Pilatus PC 9/A. Client Report AOD 96/29, Aeronautical and Maritime Research Laboratory, February 1997.

9. PEI Aerodynamics. Evaluation of stability derivatives for the PC 9/A turbo-trainer. Technical report, Pilatus Aircraft Limited, 30 July 1983.

10. J.E. Williams and Vukelich. The USAF stability and control digital DATCOM - volume I, users manual. Technical Report AFFDL-TR-76-45, Vol I, McDonnell Douglas Astronautics Company - East, St Louis, Missouri, USA, November 1976.

11. J.E. Williams and Vukelich. The USAF stability and control digital DATCOM - volume II, implementation of DATCOM methods. Technical Report AFFDL-TR-76-45, Vol II, McDonnell Douglas Astronautics Company - East, St Louis, Missouri, USA, November 1976.

12. *Statistics Toolbox User's Guide.* The MathWorks, Inc, Natick, MA, January 1997.

13. J.E. Murray and R.E. Maine. pEst version 2.1 user's manual. Technical Memorandum 8828, NASA Ames Research Center, Dryden Flight Research Facility, Edwards, CA, USA, September 1987.

14. R.E. Maine and K.W. Iliff. Maximum likelihood estimation of translational acceleration derivatives from flight data. *AIAA Journal of Aircraft*, 1979.

15. A.D. Snowden and J.S. Drobik. F-111C longitudinal and lateral aerodynamic flight data analysis for take-off and landing configurations. Technical Report 0321, DSTO–Aeronautical and Maritime Research Laboratory, Melbourne, Victoria, Australia, April 1996.

16. R.E. Maine and K.W. Iliff. User's manual for MMLE3, a general FORTRAN program for maximum likelihood parameter estimation. Technical Paper 1563, Dryden Flight Research Center, Edwards, California, USA, 1980.

17. N. van Bronswijk, P. W. Gibbens, D. M. Newman, and K. C. Wong. Investigation of the effects of propeller power on the stability and control of a tractor-propeller powered single-engined low-wing monoplane. Technical Report 9801, University of Sydney, January 1998.

18. J. P. Shivers, M. P. Fink, and G. M. Ware. Full-scale wind tunnel investigation of the static longitudinal and lateral characteristics of a light single-engine low-wing airplane. TN D-5857, National Aeronautics and Space Administration, June 1970.

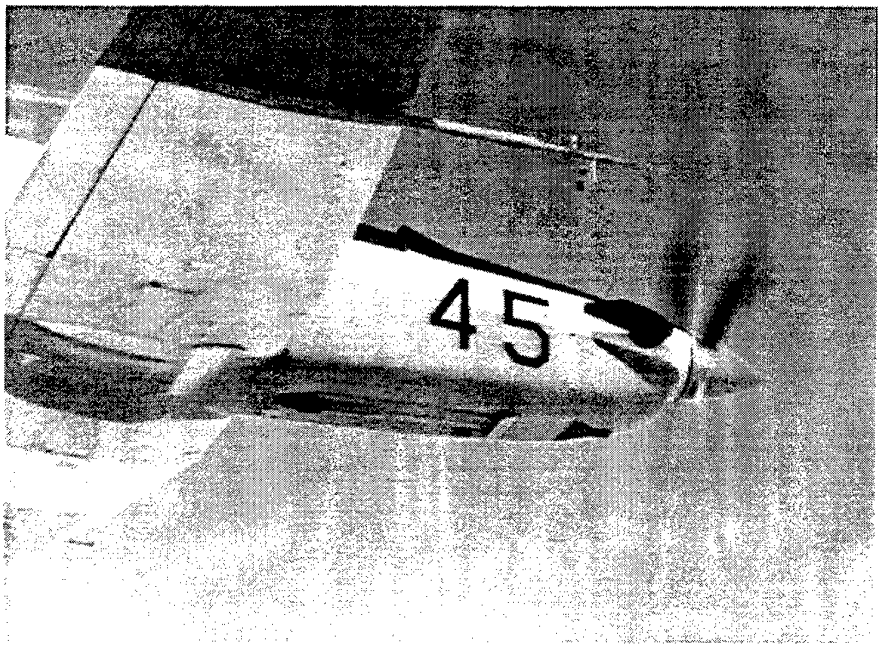

Figure 1: Air data boom installation.

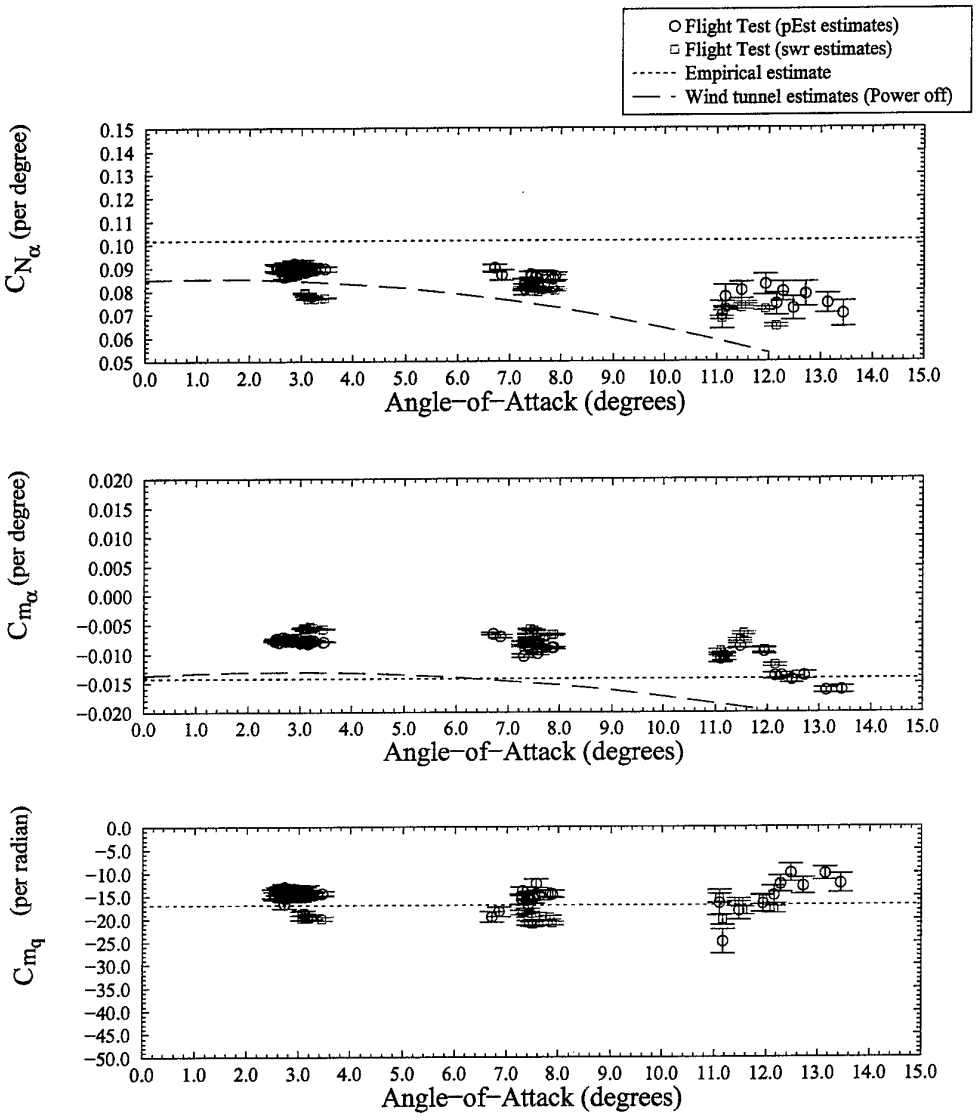

Figure 2: PC 9/A angle-of-attack and pitch rate derivatives, 3-2-1-1 manoeuvres at 5000 ft.

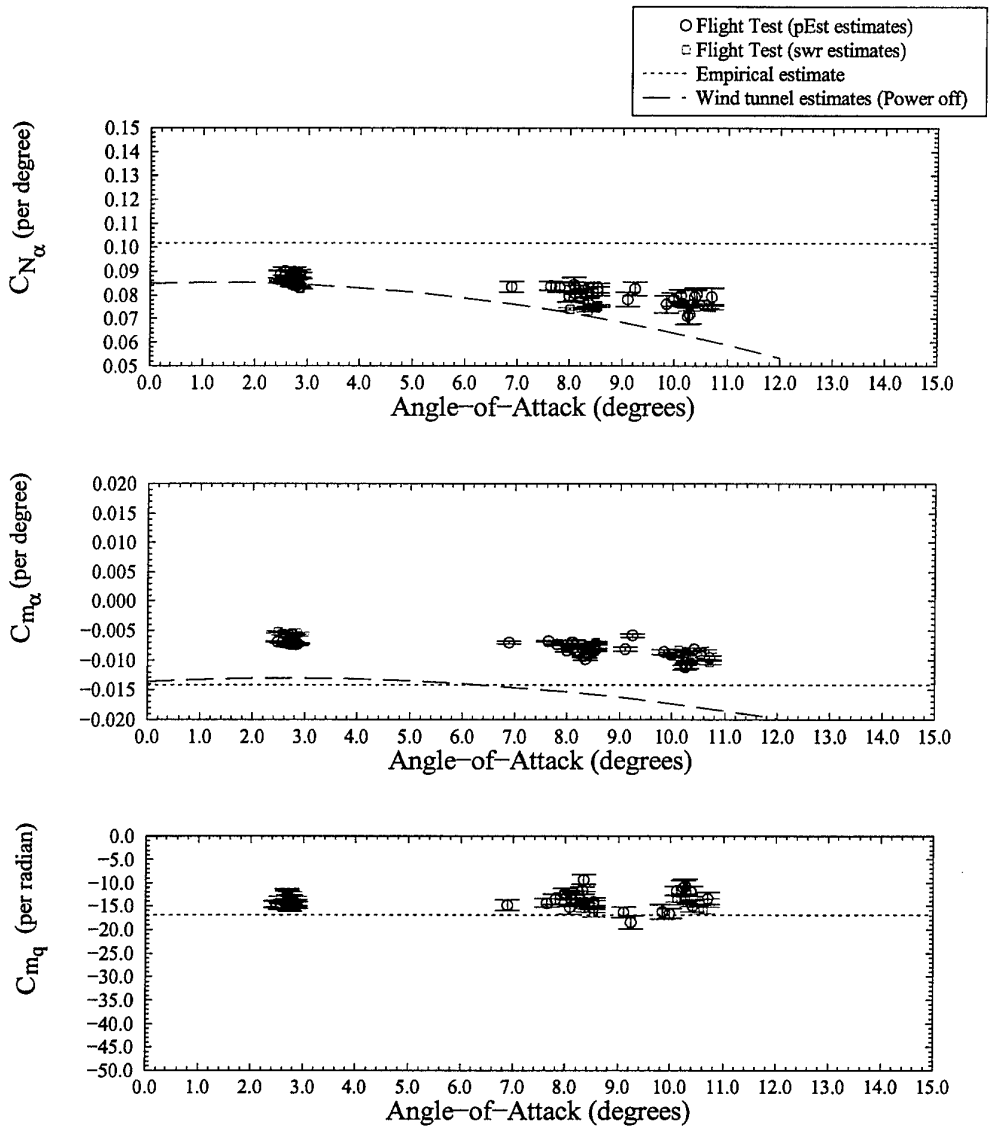

Figure 3: PC 9/A angle-of-attack and pitch rate derivatives, 3-2-1-1 manoeuvres at 10 000 ft.

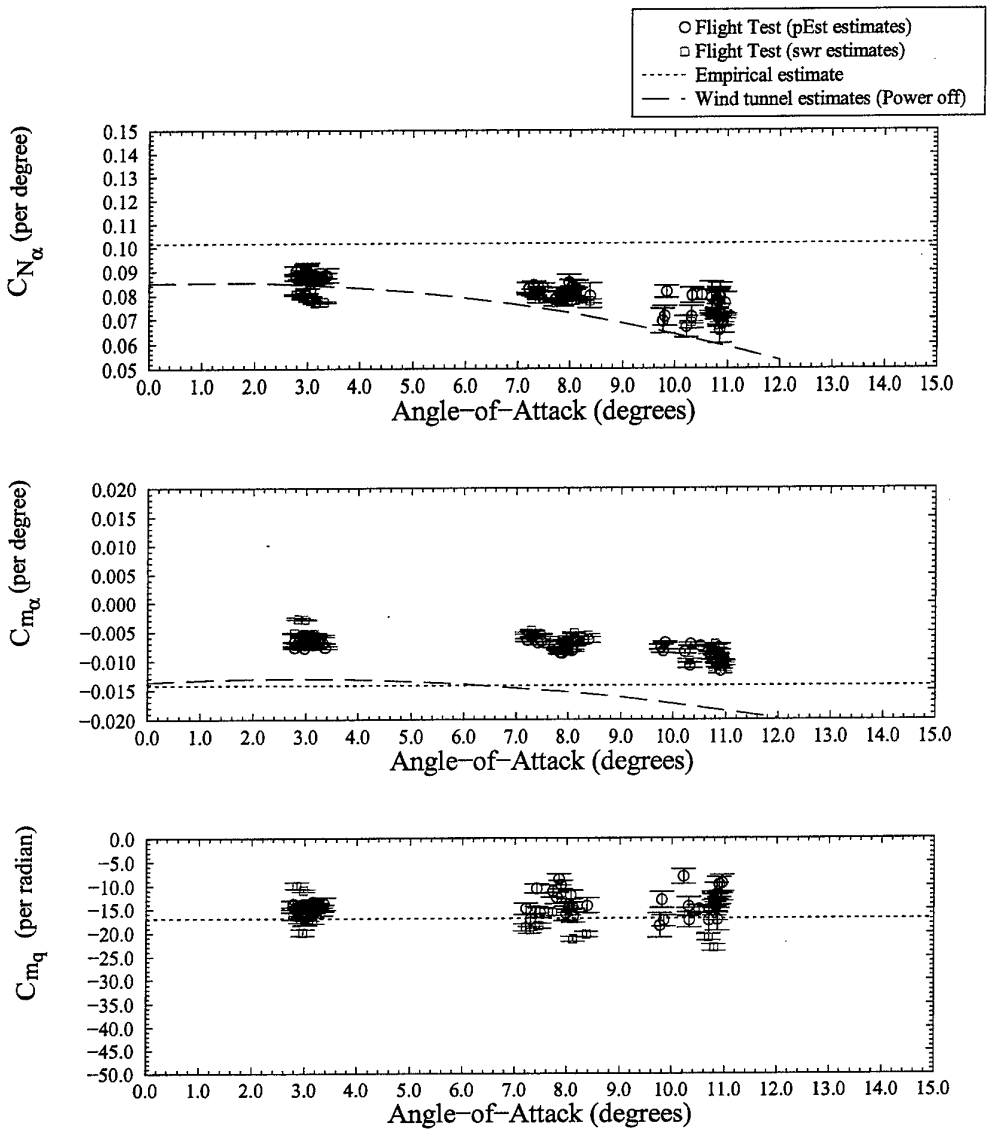

Figure 4: PC 9/A angle-of-attack and pitch rate derivatives, 3-2-1-1 manoeuvres at 15 000 ft.

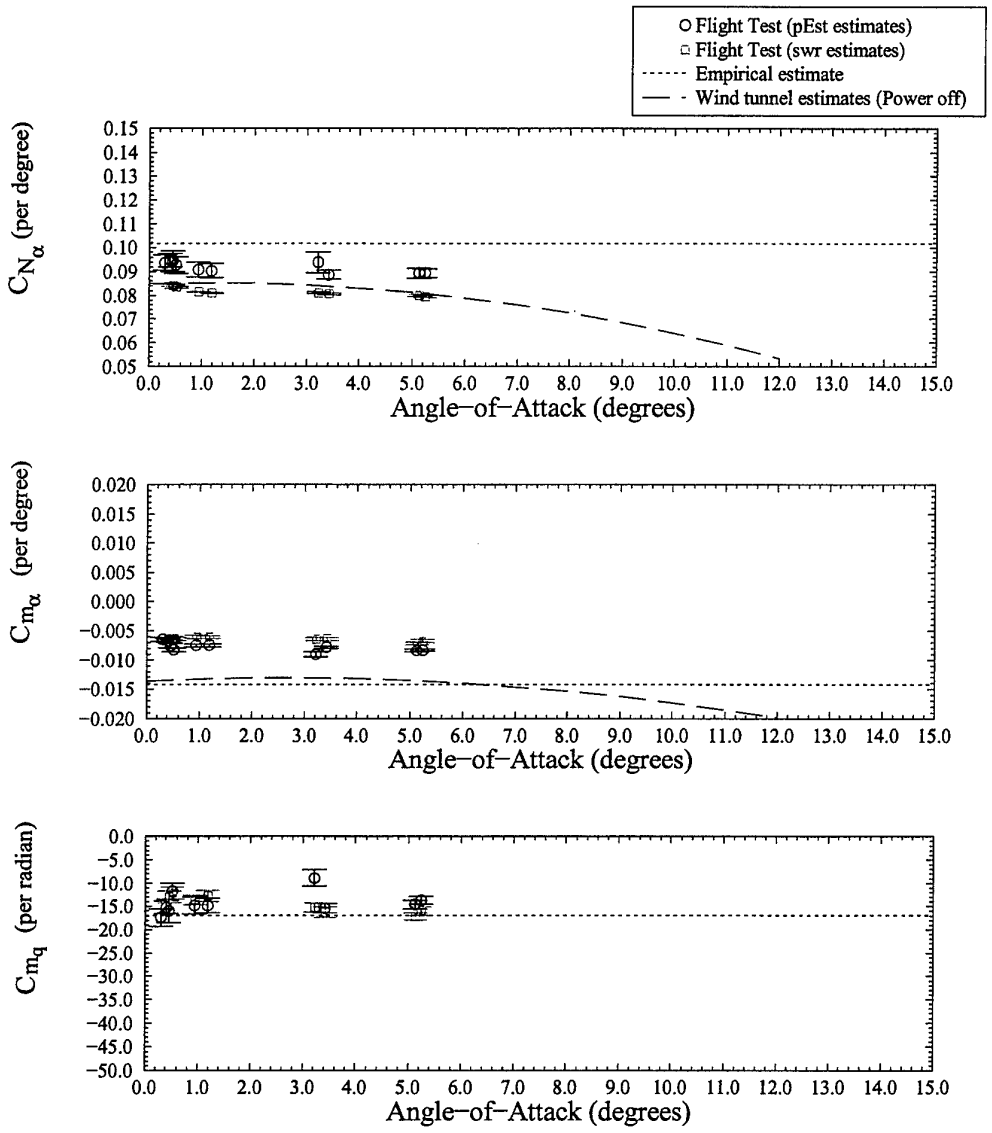

Figure 5: PC 9/A angle-of-attack and pitch rate derivatives, doublet manoeuvres at 5000 ft.

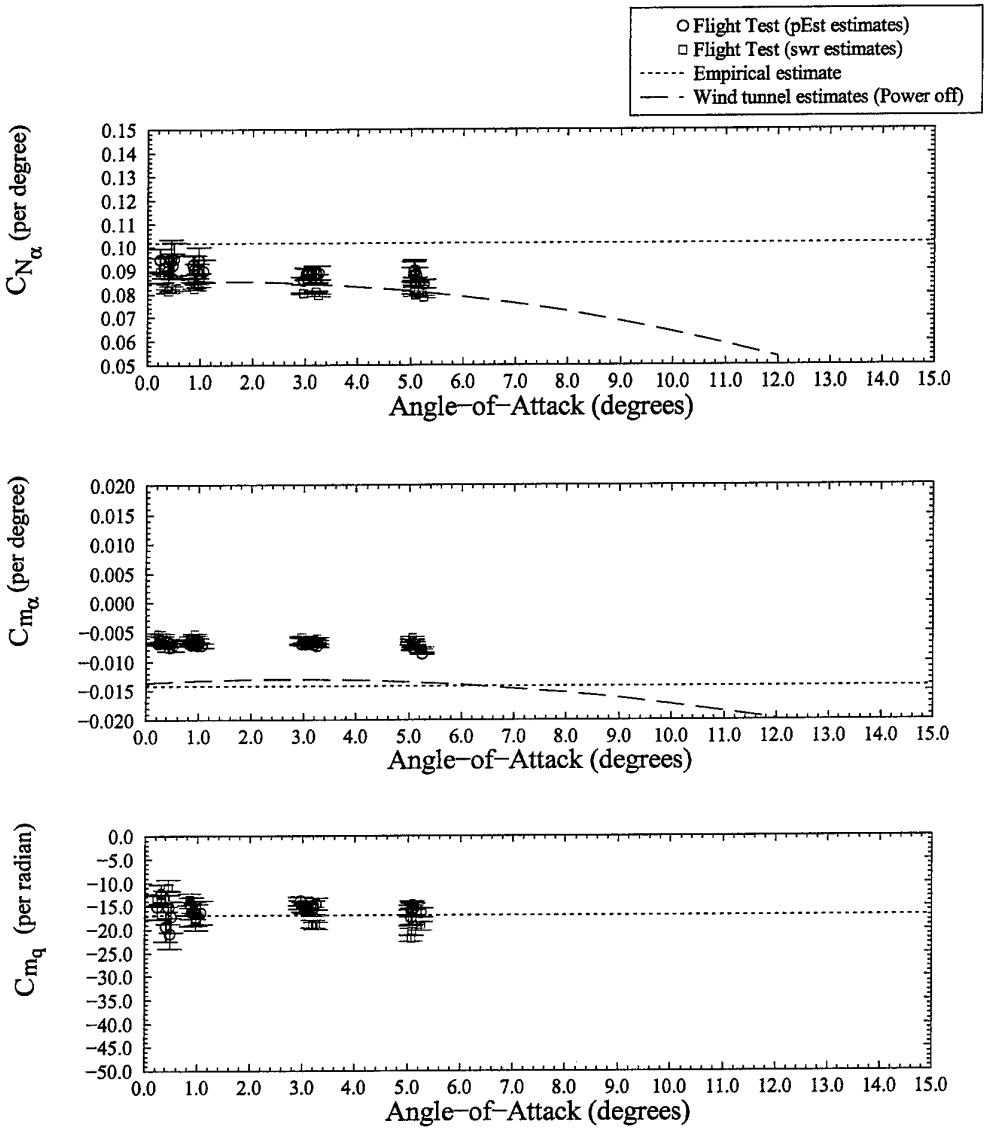

Figure 6: PC 9/A angle-of-attack and pitch rate derivatives, doublet manoeuvres at 15 000 ft.

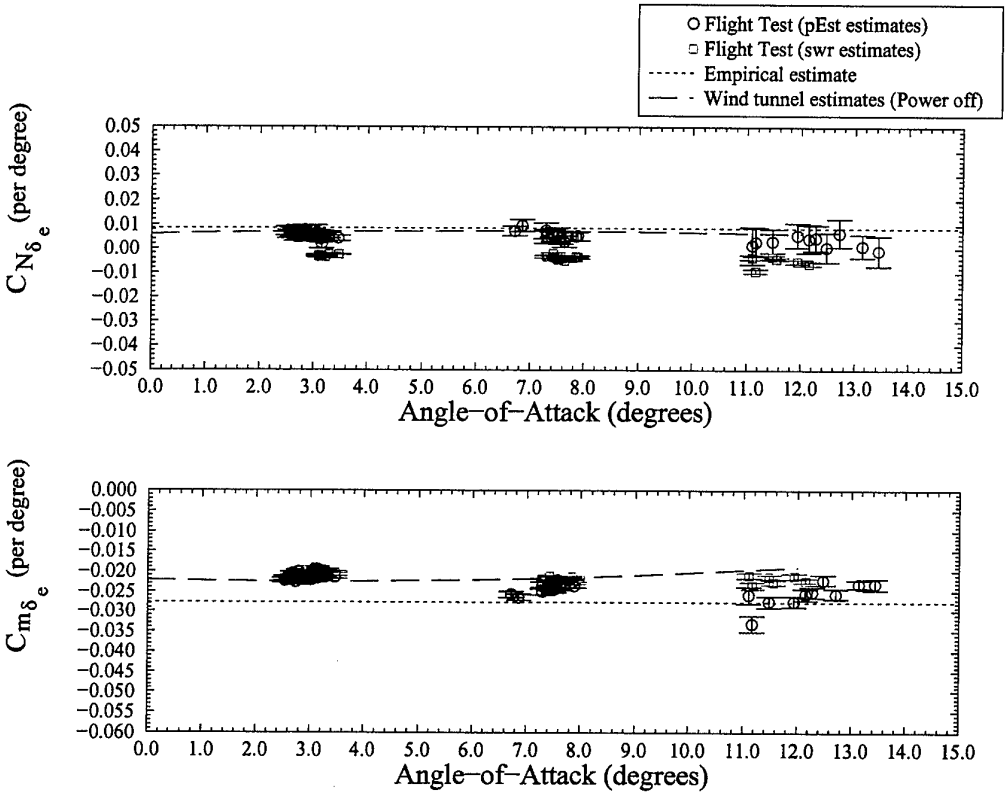

Figure 7: PC 9/A control derivatives, 3-2-1-1 manoeuvres at 5000 ft.

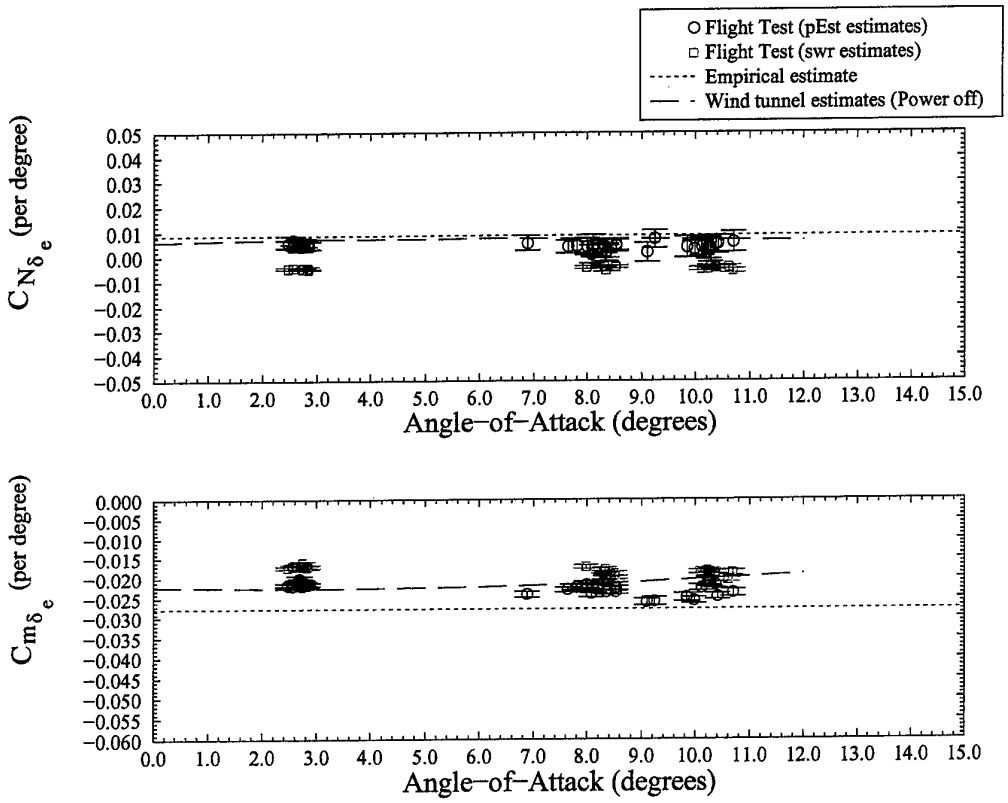

Figure 8: PC 9/A control derivatives, 3-2-1-1 manoeuvres at 10 000 ft.

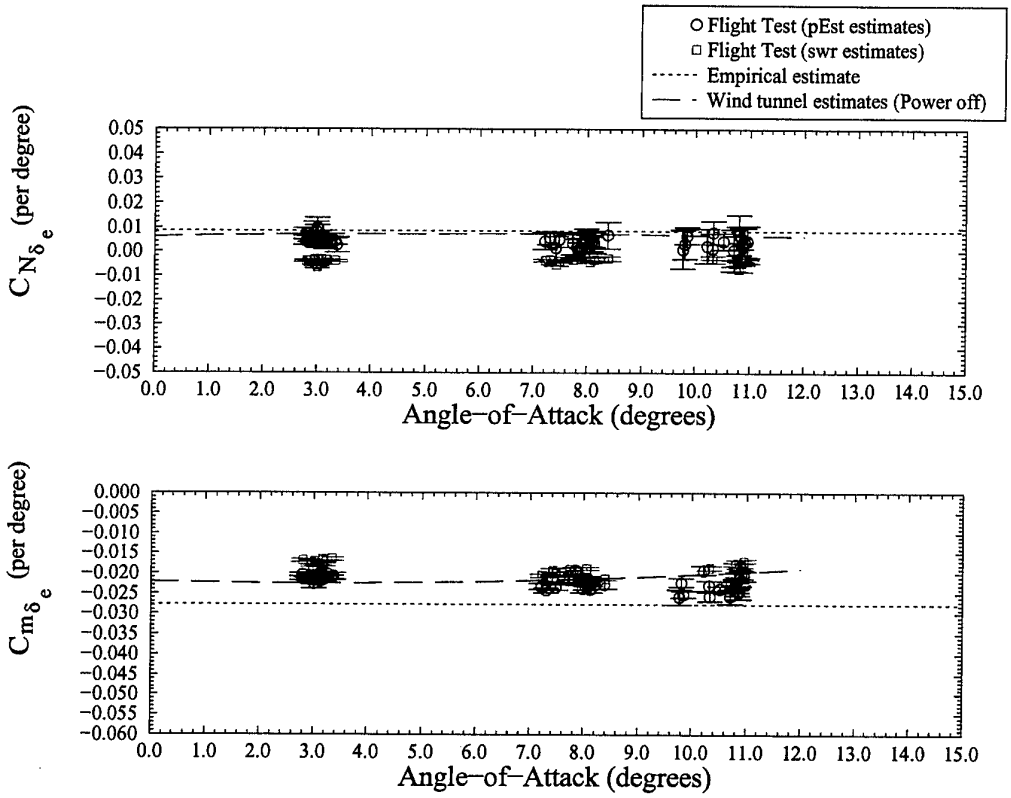

Figure 9: PC 9/A control derivatives, 3-2-1-1 manoeuvres at 15 000 ft.

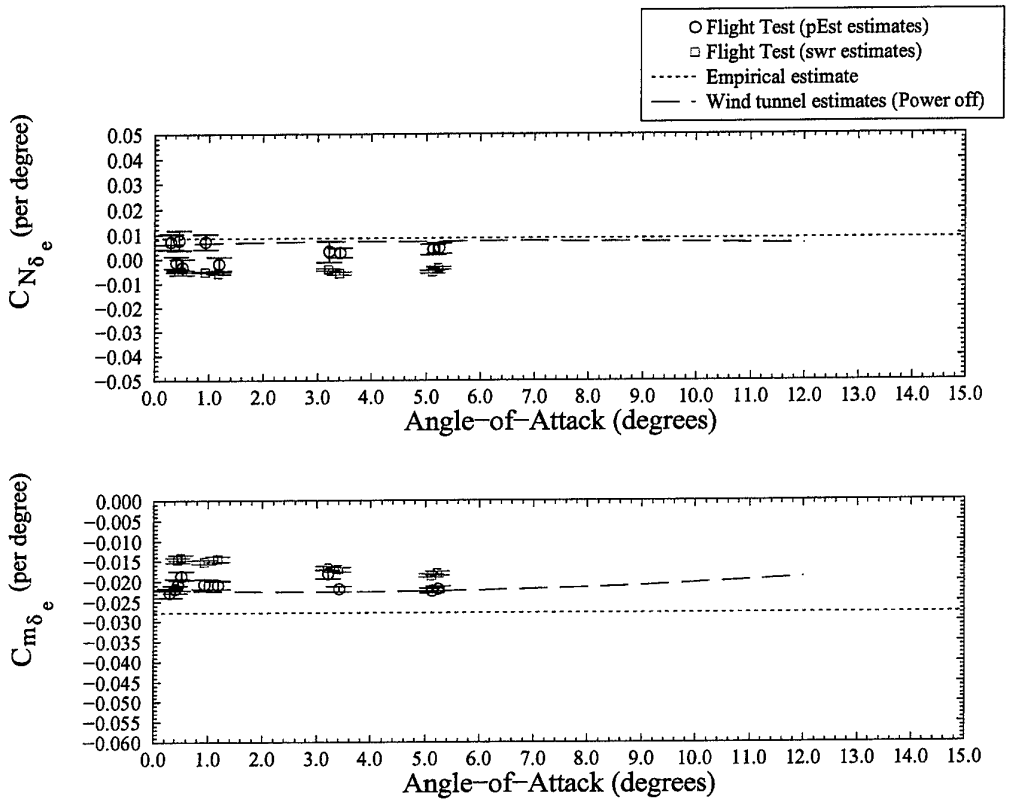

Figure 10: PC 9/A control derivatives, doublet manoeuvres at 5000 ft.

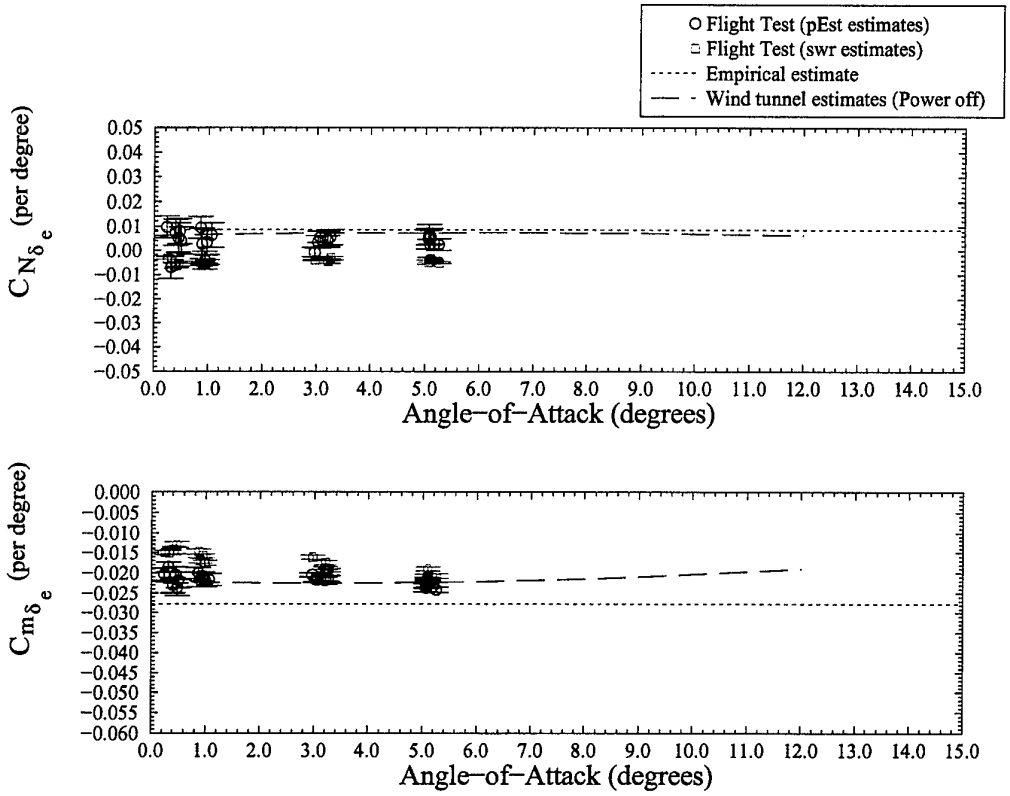

Figure 11: PC 9/A control derivatives, doublet manoeuvres at 15 000 ft.

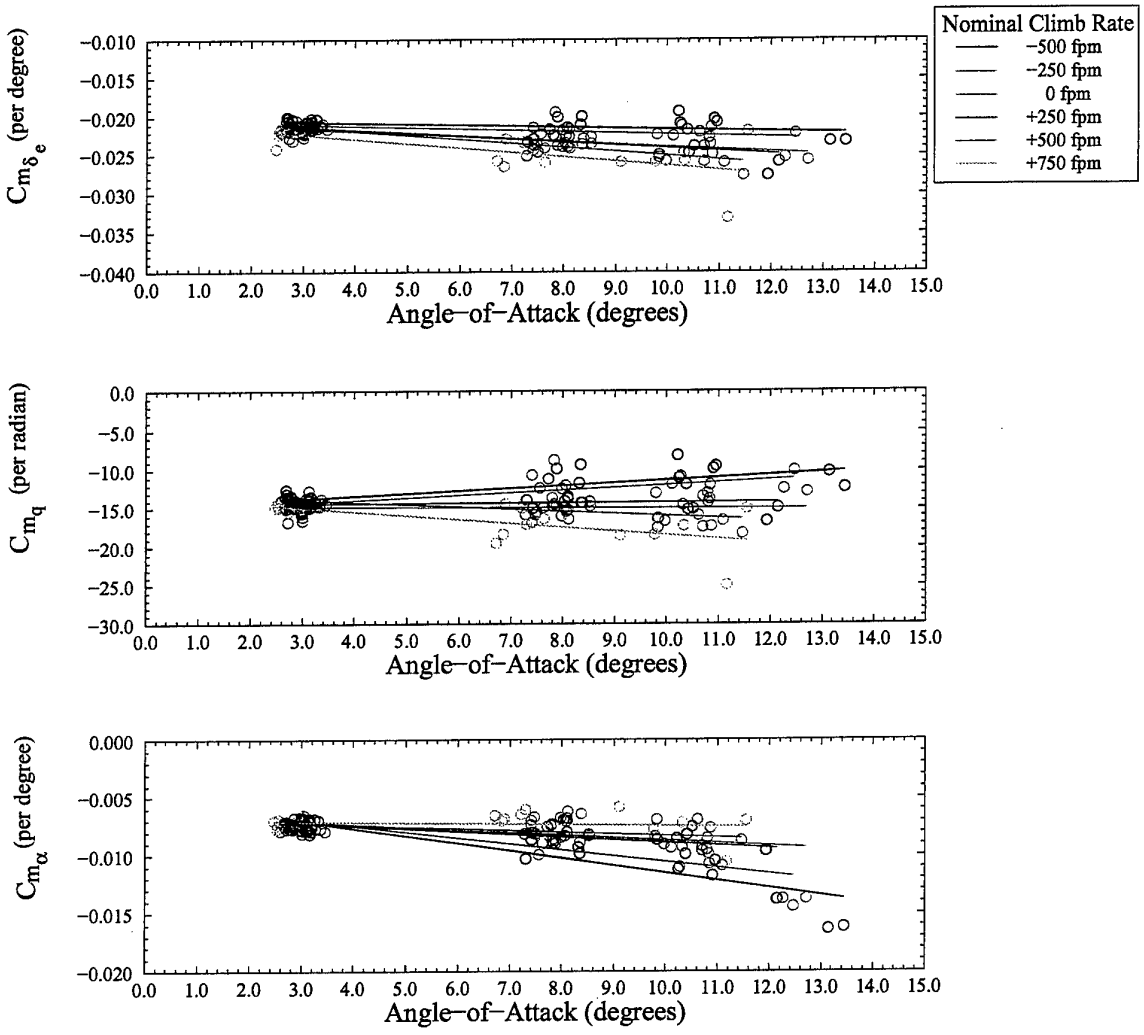

Figure 12: Variation of C_m derivatives with nominal rate of climb.

Appendix A: Weight, Centre-of-Gravity and Mass Moments-of-Inertia

The aircraft mass, centre-of-gravity and mass moments-of-inertia were determined for each test manoeuvre based on the aircraft fuel mass. The basic aircraft, pilot and fuel masses and moment arms from references [2] and [3] are given in table A1. The moment arms are measured relative to the aircraft datum, located 3m forward of the engine firewall, and 2m below the forward fuselage reference plane.

	Mass (kg)	Moment Arm (m)
Basic Aircraft	1784.5	4.306
Pilot	81.6	4.061
Fuel	Variable	4.178

Table A1: Flight test aircraft mass distribution [2, 3].

The mass of the aircraft is calculated as the sum of the basic aircraft, pilot and remaining fuel masses, by the following equation.

$$M = 1866.1 + M_F \quad \text{(kg)} \tag{A1}$$

The longitudinal centre-of-gravity position of the flight test aircraft was determined from the following equation.

$$x_{c.g.} = \frac{8015.5+4.178M_F}{1866.1+M_F} \quad \text{(M)} \tag{A2}$$

During the flight test program, the aircraft longitudinal centre-of-gravity position varied between 4.27 m (24.2%MAC) and 4.30 m (25.6%MAC). The lateral and vertical centre-of-gravity positions were assumed to be invariant with fuel usage, and were fixed at values of 0.024m and -2.2 m, respectively, relative to the aircraft datum.

The mass moments-of-inertia of the aircraft are given by the following equations.

$$I_{XX} = 2505.9 + 6.177\,(M - 1866.1) \quad (\text{kg.m}^2) \tag{A3}$$

$$I_{YY} = 6622.2 + 0.033\,(M - 1866.1) \quad (\text{kg.m}^2) \tag{A4}$$

$$I_{ZZ} = 8467.1 + 6.188\,(M - 1866.1) \quad (\text{kg.m}^2) \tag{A5}$$

$$I_{XY} = 49.0 + 0.0057\,(M - 1866.1) \quad (\text{kg.m}^2) \tag{A6}$$

$$I_{XZ} = 196.9 + 0.0041\,(M - 1866.1) \quad (\text{kg.m}^2) \tag{A7}$$

$$I_{YZ} = 3.0 + 0.0007\,(M - 1866.1) \quad (\text{kg.m}^2) \tag{A8}$$

Appendix B: C_{N_q} Contribution to Total C_N Equation

Data analysis carried out previously on the PC 9/A and other aircraft, has consistently highlighted the difficulty of obtaining reasonable estimates for the normal force due to pitch rate derivative, C_{N_q}. In the past, the derivative C_{N_q} was usually fixed at some *a priori* value whilst the remaining derivatives were estimated. The opportunity was taken to further investigate the effect that fixing C_{N_q} would have on the other derivatives. This investigation was done in two parts. First, the total contribution of the pitch rate derivative to the total normal force coefficient was determined. Then, the effect of changes in C_{N_q} on the maximum likelihood estimates of the remaining derivatives was examined.

The normal force coefficient may be represented by the following equation:

$$C_N = C_{N_0} + C_{N_\alpha}\alpha + C_{N_q}\frac{q\bar{c}}{2V} + C_{N_{\delta_e}}\delta_e \tag{B1}$$

The contribution of the pitch rate, q, on the normal force coefficient of the PC 9/A was determined by comparing the relative sizes of each component in the above equation for a sample case. Those results are shown in figure B1 and it can be seen that changes in the normal force coefficient are mainly due to changes in the aircraft angle-of-attack and that the contribution of the pitch rate is relatively small.

The effect of error in the *a priori* estimate of C_{N_q} was investigated by changing the value of C_{N_q} and examining the changes in the other derivatives. Results from the sample case are shown in table B1 and they show that changes in C_{N_q} appear to have little effect on most of the derivatives with the exception of $C_{N_{\delta_e}}$. This derivative shows considerable variation with C_{N_q}, which was to be expected. Figure B1 shows, however, that like the C_{N_q} derivative, $C_{N_{\delta_e}}$ has only a small contribution to the total normal force coefficient. Hence the effect of any errors present in the *a priori* estimate of C_{N_q} should be minimal.

C_{N_q}	-16.0	-8.00	0.00	7.96	8.00	16.00
C_{N_0}	8.44E-02	9.56E-02	1.07E-01	1.18E-01	1.18E-01	1.29E-01
C_{N_α}	8.56E-02	8.39E-02	8.24E-02	8.08E-02	8.08E-02	8.79E-02
$C_{N_{\delta_e}}$	-1.11E-02	-8.39E-03	-8.24E-03	-4.31E-03	-4.50E-03	-4.32E-03

Table B1: Effect of C_{N_q} variation on C_N equation components.

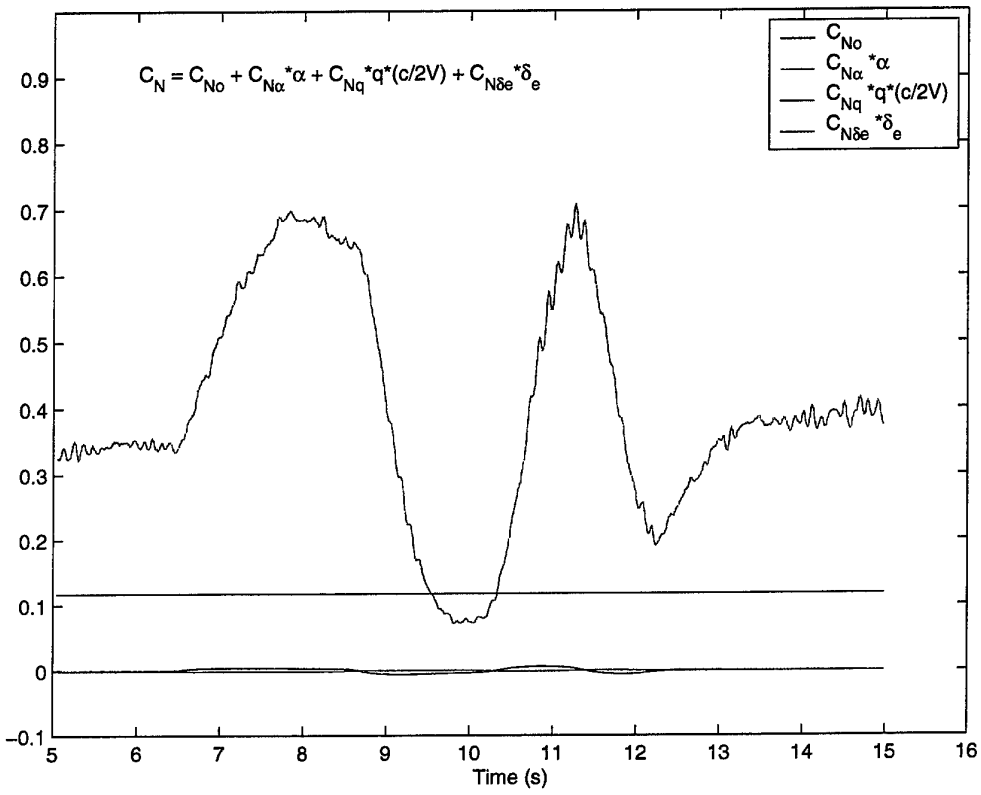

Figure B1: Relative magnitudes of C_N equation components.

DISTRIBUTION LIST

A Correlation between Flight-determined Longitudinal Derivatives and Ground-based Data for the Pilatus PC 9/A Training Aircraft in Cruise Configuration

Andrew D. Snowden, Hilary A. Keating, Nick van Bronswijk and Jan S. Drobik

	Number of Copies
DEFENCE ORGANISATION	
Task Sponsor	
COPS HQAC	1
S&T Program	
Chief Defence Scientist FAS Science Policy AS Science Corporate Management	1
Director General Science Policy Development	1
Counsellor, Defence Science, London	Doc Data Sht
Counsellor, Defence Science, Washington	Doc Data Sht
Scientific Adviser to MRDC Thailand	Doc Data Sht
Scientific Adviser Policy and Command	1
Navy Scientific Adviser	Doc Data Sht
Scientific Adviser, Army	Doc Data Sht
Air Force Scientific Adviser	1
Director Trials	1
Aeronautical and Maritime Research Laboratory	
Director, Aeronautical and Maritime Research Laboratory	1
Air Operations Division	
Chief, Air Operations Division	1
Research Leader, Avionics and Flight Mechanics	1
Head, Flight Mechanics Applications	1
Task Manager - G. J. Brian	1
Author - A. D. Snowden	1
Author - H. A. Keating	1
Author - N. van Bronswijk	1
Author - J. S. Drobik	1
B. A. Woodyatt	1
K. L. Bramley	1
DSTO Libraries	
Library Fishermans Bend	1

Library Maribyrnong	1
Library Salisbury	2
Library, MOD, Pyrmont	Doc Data Sht
US Defense Technical Information Center	2
UK Defence Research Information Centre	2
Canada Defence Scientific Information Service	1
NZ Defence Information Centre	1
National Library of Australia	1
Capability Systems Staff	
Director General Maritime Development	Doc Data Sht
Director General C3I Development	Doc Data Sht
Director General Aerospace Development	1
Aircraft Research and Development Unit	
MSSUP1	1
Intelligence Program	
DGSTA Defence Intelligence Organisation	1
Manager, Information Centre, Defence Intelligence Organisation	1
Corporate Support Program (libraries)	
Officer in Charge, TRS, Defence Regional Library, Canberra	1
UNIVERSITIES AND COLLEGES	
Australian Defence Force Academy Library	1
Head of Aerospace and Mechanical Engineering, ADFA	1
Deakin University Library, Serials Section (M List)	1
Librarian, Flinders University	1
Head of Aeronautical Engineering, University of Sydney	1
Head of Centre of Expertise in Aerodynamic Loading, RMIT	1
Adrian Pearce, Computer Science, Curtin University WA	1
OTHER ORGANISATIONS	
NASA (Canberra)	1
Info Australia	1
ABSTRACTING AND INFORMATION ORGANISATIONS	
Library, Chemical Abstracts Reference Service	1
Engineering Societies Library, US	1

Materials Information, Cambridge Science Abstracts, US	1
Documents Librarian, The Center for Research Libraries, US	1

INFORMATION EXCHANGE AGREEMENT PARTNERS

Acquisitions Unit, Science Reference and Information Service, UK	1
Library – Exchange Desk, National Institute of Standards and Technology, US	1
National Aerospace Library, Japan	1
National Aerospace Library, Netherlands	1

SPARES

A. D. Snowden	5

Total number of copies:	55

DEFENCE SCIENCE AND TECHNOLOGY ORGANISATION DOCUMENT CONTROL DATA				1. CAVEAT/PRIVACY MARKING
2. TITLE A Correlation between Flight-determined Longitudinal Derivatives and Ground-based Data for the Pilatus PC 9/A Training Aircraft in Cruise Configuration			3. SECURITY CLASSIFICATION Document (U) Title (U) Abstract (U)	
4. AUTHOR(S) Andrew D. Snowden, Hilary A. Keating, Nick van Bronswijk and Jan S. Drobik			5. CORPORATE AUTHOR Aeronautical and Maritime Research Laboratory 506 Lorimer St, Fishermans Bend, Victoria, Australia 3207	
6a. DSTO NUMBER DSTO–TR–0937	6b. AR NUMBER AR-011-205		6c. TYPE OF REPORT Technical Report	7. DOCUMENT DATE February, 2000
8. FILE NUMBER M1/9/700	9. TASK NUMBER AIR 97/135	10. SPONSOR COPS HQAC	11. No OF PAGES 26	12. No OF REFS 18
13. DOWNGRADING / DELIMITING INSTRUCTIONS Not Applicable			14. RELEASE AUTHORITY Chief, Air Operations Division	
15. SECONDARY RELEASE STATEMENT OF THIS DOCUMENT *Approved For Public Release* OVERSEAS ENQUIRIES OUTSIDE STATED LIMITATIONS SHOULD BE REFERRED THROUGH DOCUMENT EXCHANGE, PO BOX 1500, SALISBURY, SOUTH AUSTRALIA 5108				
16. DELIBERATE ANNOUNCEMENT No Limitations				
17. CITATION IN OTHER DOCUMENTS No Limitations				
18. DEFTEST DESCRIPTORS Flight tests Royal Australian Air Force Fixed wing			PC 9/A aircraft Flight dynamics	
19. ABSTRACT A series of flight tests were conducted on the PC 9/A aircraft, A23-045, at the Royal Australian Air Force's Aircraft Research and Development Unit. System identification techniques were applied to the data obtained from these flight tests to determine the stability and control derivatives of the aircraft. The longitudinal results for the aircraft in cruise configuration are presented in this report and comparisons are made with empirical and ground based estimates.				